

Cavity Sideband Cooling of a Single Trapped Ion

David R. Leibrandt,* Jaroslaw Labaziewicz, Vladan Vuletić, and Isaac L. Chuang

*Department of Physics & Center for Ultracold Atoms Massachusetts Institute of Technology,
77 Massachusetts Avenue, Cambridge, Massachusetts, 02139, USA*

(Received 1 May 2009; published 31 August 2009)

We report a demonstration and quantitative characterization of one-dimensional cavity cooling of a single trapped $^{88}\text{Sr}^+$ ion in the resolved-sideband regime. We measure the spectrum of cavity transitions, the rates of cavity heating and cooling, and the steady-state cooling limit. The cavity cooling dynamics and cooling limit of 22.5(3) motional quanta, limited by the moderate coupling between the ion and the cavity, are consistent with a simple model [Phys. Rev. A **64**, 033405 (2001)] without any free parameters, validating the rate equation model for cavity cooling.

DOI: 10.1103/PhysRevLett.103.103001

PACS numbers: 37.10.Rs, 37.10.Ty, 37.30.+i

Cooling atoms, molecules, and even macroscopic objects to the quantum mechanical ground state of their motion represents an important step towards comprehensive control of large or complex quantum mechanical systems [1–4]. Of particular interest are cooling methods that do not destroy the quantum mechanical coherences in other degrees of freedom. For example, in trapped ion quantum information processing [5], it is necessary to cool the motion of the ions to the ground state without affecting the internal state where the quantum information is stored. This has been accomplished by sympathetic cooling of the processing ion using a laser cooled ion of another species [6].

An all optical method that may allow one to cool a particle without causing decoherence of the internal states is cavity cooling. When a particle is illuminated with monochromatic laser light, the spectrum of the scattered light is distributed around the incident frequency due to the particle's motion. If an optical resonator is used to enhance selected portions of the emission spectrum, such that the average emission frequency is larger than that of the incident light, energy conservation implies that the particle is cooled in the scattering process (cavity cooling) [7–9]. Unlike conventional Doppler cooling [10], cavity cooling does not require the incident light to be matched to an atomic resonance, and can in principle be performed with nonresonant light. As light scattered far off resonance carries no information about the atom's internal state [11,12], such a process can potentially cool an atom without destroying a quantum superposition of internal states.

Cavity cooling relies on the frequency discrimination provided by the resonator, and hence cooling to the quantum mechanical ground state of the external trapping potential is possible only when the trap frequency ω exceeds the cavity linewidth κ (cavity resolved-sideband regime) [9]. In the resolved-sideband regime cooling is achieved by tuning the resonator an amount ω to the blue of the incident light, such that scattering events into the cavity correspond to transitions $|n\rangle \rightarrow |n-1\rangle$ that lower the motional quan-

tum number n . The steady-state temperature is then set by the competition between cooling by photons scattered into the cavity and recoil heating by photons scattered into free-space [9]. Denoting the probability of scattering into a resonant cavity relative to free-space by the cooperativity η , the steady-state average vibrational quantum number n_∞ in the resolved-sideband regime $\kappa \ll \omega$ is given by [9]

$$n_\infty = \left(\frac{\kappa}{4\omega}\right)^2 + \frac{C}{\eta} \left[1 + \left(\frac{\kappa}{4\omega}\right)^2\right], \quad (1)$$

where C is a dimensionless factor of order unity that depends on the cooling geometry. Thus in the strong-coupling regime $\eta \gg 1$ cooling to the motional ground state is possible, while for moderate coupling $\eta \lesssim 1$ the cooling is limited by the cooperativity to $n_\infty = C/\eta$.

Cavity cooling has been demonstrated in the weak-confinement regime $\kappa \gg \omega$ with single trapped atoms without directly measuring the atomic temperature [13–15] and with atomic ensembles in a different parameter regime of collective coupling [16,17]. In this work, using a single trapped $^{88}\text{Sr}^+$ ion in the resolved-sideband regime, we measure for the first time cavity heating and cooling rates and the steady-state cooling limit, and observe parameter-free agreement with a rate equation model for cavity cooling [9].

This experiment (Fig. 1) builds on the pioneering cavity cooling work with neutral atoms in the weak-confinement regime [13–17] using the exquisite experimental control and strong confinement of trapped ions [18–21]. A single $^{88}\text{Sr}^+$ ion is confined in a linear RF Paul trap with motional frequencies $\omega_{x,y,z} = 2\pi \times (1.45, 1.20, 0.87)$ MHz. The cavity is 5 cm long and has a finesse $F = 2.56(1) \times 10^4$, resulting in a cavity linewidth (energy decay rate constant) $\kappa = 2\pi \times 117(1)$ kHz. The cavity is typically detuned by a few tens of MHz from the $S_{1/2} \leftrightarrow P_{1/2}$ transition, which has a wavelength $\lambda = 422$ nm and a population decay rate $\Gamma = 2\pi \times 20.2$ MHz. The optical cavity is oriented along the ion trap axis and the 422 nm cavity cooling laser is perpendicular to the ion trap axis. A portion of the cavity

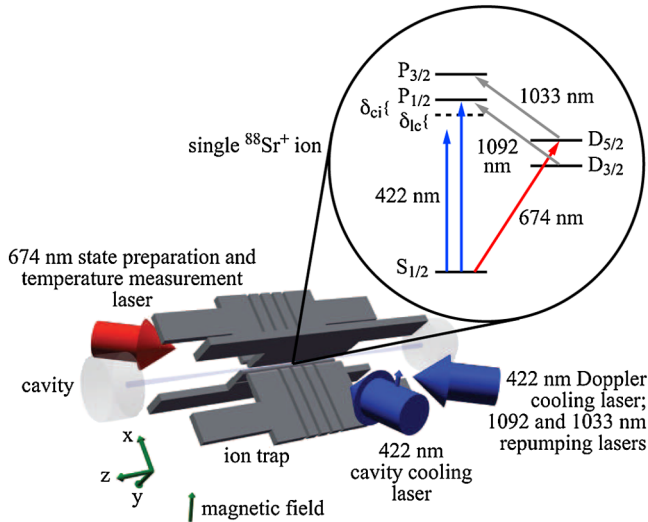


FIG. 1 (color online). Schematic of the experimental setup. A single $^{88}\text{Sr}^+$ ion is confined in the center of a linear RF Paul trap and coupled to an optical resonator oriented along the trap axis. The inset shows the ion energy levels (solid lines) and the cavity resonance (dashed line).

cooling laser is frequency shifted by 9.175 GHz (roughly three cavity free spectral ranges) and injected into the cavity TEM₁₁ mode to lock the cavity length to the cavity cooling laser via the Pound-Drever-Hall method. The additional 422 nm Doppler cooling laser, 1033 nm and 1092 nm repumpers, and 674 nm state preparation and temperature measurement laser are all at 45 degrees to the trap axis such that they have projections along all of the ion motional principal axes. A 4.1 G magnetic field is applied to define the quantization axis. The cooperativity at an antinode of the cavity for a two-level atom, given by the product of cavity mode solid angle [$\propto 1/(k^2 w_0^2)$] and average number of photon round-trips ($\propto F$), is $\eta_0 = 24F/(\pi k^2 w_0^2) = 0.26$, where $k = 2\pi/\lambda$ is the wave number and $w_0 = 57.9(6)\ \mu\text{m}$ the radius of the cavity TEM₀₀ mode waist [9].

The effective cooperativity is reduced from the cooperativity of a two-level atom η_0 by several effects, including the reduced dipole matrix element for π polarized light on the $^{88}\text{Sr}^+ S_{1/2} \leftrightarrow P_{1/2}$ transition (0.31), the error in positioning the ion in the center of the cavity mode (0.89), the nonzero laser linewidth (0.82), and the ion's thermal motion (0.32 for our typical temperature). The combination of these independently measured effects results in a calculated effective cooperativity $\eta = 0.019$. We determine η experimentally by comparing the photon scattering rate by the ion into the resonant cavity Γ_c (detuning between incident laser and cavity $\delta_{lc} = 0$) to the scattering rate Γ_{sc} into free-space. The two scattering rates are measured simultaneously by two photon-counting photomultiplier tubes located at the output of the cavity and above the ion trap in the $(\hat{x} - \hat{y})/\sqrt{2}$ direction, respectively. The free-space scatter collection efficiency is calibrated by optically

pumping the ion into the $D_{3/2}$ state by turning off the 1092 nm laser, then turning off the 422 nm laser and collecting the 422 nm fluorescence while repumping with the 1092 nm laser. The thus measured light collection efficiency is independent of the laser intensity at the ion. Figure 2 shows the results of the cooperativity measurement for several values of the cavity-ion detuning δ_{ci} with the ion located at an antinode. The slope $d\Gamma_c/d\Gamma_{sc}$ at small values of Γ_{sc} is the effective cooperativity $\eta = 0.018(4)$, consistent with our calculated value. The saturation behavior of Fig. 2 at large Γ_{sc} is due to the finite repumping rate from the metastable $D_{3/2}$ state, which frequency broadens the scattered light, and reduces the spectral overlap with the cavity mode.

Because of the symmetries of the light-ion interaction, there are selection rules for the motional sideband transitions that depend on the location of the ion in the cavity standing wave [16,20,22]. The cavity scattering process is a two-photon transition where a photon is absorbed from the traveling-wave cooling laser and another photon emitted into the cavity. The momentum transfer in the scattering process enables the coupling between different ion motional states. Transitions which change the vibrational quantum number along the x or y directions perpendicular to the resonator ($\Delta n_{x,y} \neq 0$, enabled by the momentum of the absorbed photon) are strongest when the ion is located at an antinode, since this position corresponds to the strongest ion-cavity coupling. On the other hand, for vibration-changing transitions along z that rely on the momentum of the emitted photon, the symmetry of the standing-wave

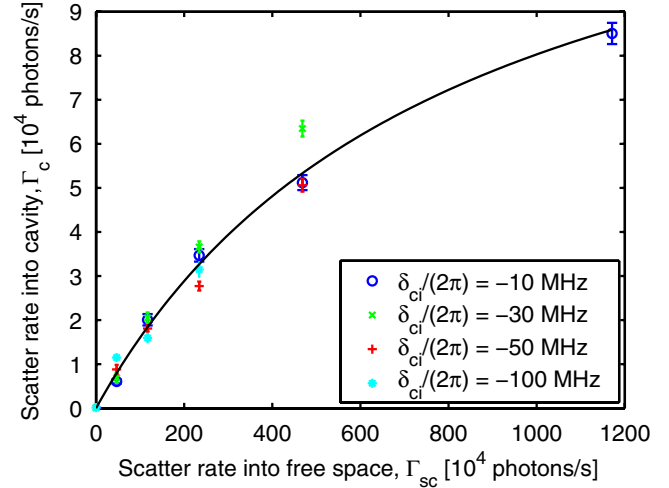


FIG. 2 (color online). Photon scattering rate Γ_c into the resonant cavity ($\delta_{lc} = 0$) as a function of the scattering rate into free-space Γ_{sc} for several values of cavity-ion detuning δ_{ci} . Each data point is measured by preparing the ion at fixed temperature by Doppler cooling for 200 μs , then measuring the photon scattering rates for 50 μs . The line is a fit to the form $\Gamma_c = \eta\Gamma_{sc}/(1 + \Gamma_{sc}/\Gamma_{sat})$ with fit parameters $\eta = 0.018(4)$ and $\Gamma_{sat} = 8(2) \times 10^6 \text{ photons/s}$.

field does not allow Δn_z -even processes ($\Delta n_z = 0, \pm 2, \dots$) to occur at a node, nor Δn_z -odd processes ($\Delta n_z = \pm 1, \pm 3, \dots$) at an antinode. Consequently the relative strength of different motional transitions depends on the ion's location in the cavity, as shown in Fig. 3. When the laser-cavity detuning δ_{lc} is varied at fixed cavity-ion detuning $\delta_{ci}/(2\pi) = -60$ MHz, the scattering into the cavity reveals all three first-order motional sideband transitions ($\Delta n = \pm 1$), as well as some of the second-order

motional sideband transitions. The best cooling along the z direction as investigated here is achieved via the $\Delta n_z = -1$ transition when the atom is located at a cavity node.

We investigate one-dimensional cavity cooling along the z direction by measuring separately the recoil heating rate, as well as the cavity cooling and heating rates for pumping on the cavity red ($\delta_{lc} = -\omega_z$) and blue ($\delta_{lc} = +\omega_z$) motional sidebands, respectively. To realize a situation that allows simple quantitative comparison with the theoretical model for cavity cooling [8,9], we prepare the ion in its motional ground state by standard sideband cooling on the narrow $S_{1/2}, m = -1/2 \leftrightarrow D_{5/2}, m = -5/2$ transition. We then apply the cavity cooling laser for a variable time t with detunings $\delta_{lc} = 0$ or $\delta_{lc} = \pm\omega_z$ and $\delta_{ci}/(2\pi) = -10$ MHz. Finally, the mean vibrational quantum number $\langle n_z \rangle$ is determined by measuring the Rabi frequencies of the red and blue motional sidebands of the $S_{1/2}, m = -1/2 \leftrightarrow D_{5/2}, m = -5/2$ transition [5]. This cavity-ion detuning is near the optimum value for conventional Doppler cooling, but the geometry of the setup dictates that the cavity cooling laser Doppler cools the x and y motional modes to maintain them at $\langle n_{x,y} \rangle \leq 10$ but does not Doppler cool the z motional mode. The ion position is locked to a node of the cavity standing wave for this measurement by applying dc compensation voltages to the trap electrodes. The recoil heating rate is the slope $d\langle n_z \rangle/dt$ for $\delta_{lc} = 0$ (Fig. 4, green line), and the cavity cooling and heating rates are the differences of the slopes $d\langle n_z \rangle/dt$ for $\delta_{lc} = \pm\omega_z$ (Fig. 4, red and blue lines) and the recoil heating rate. The signature of cavity cooling is that

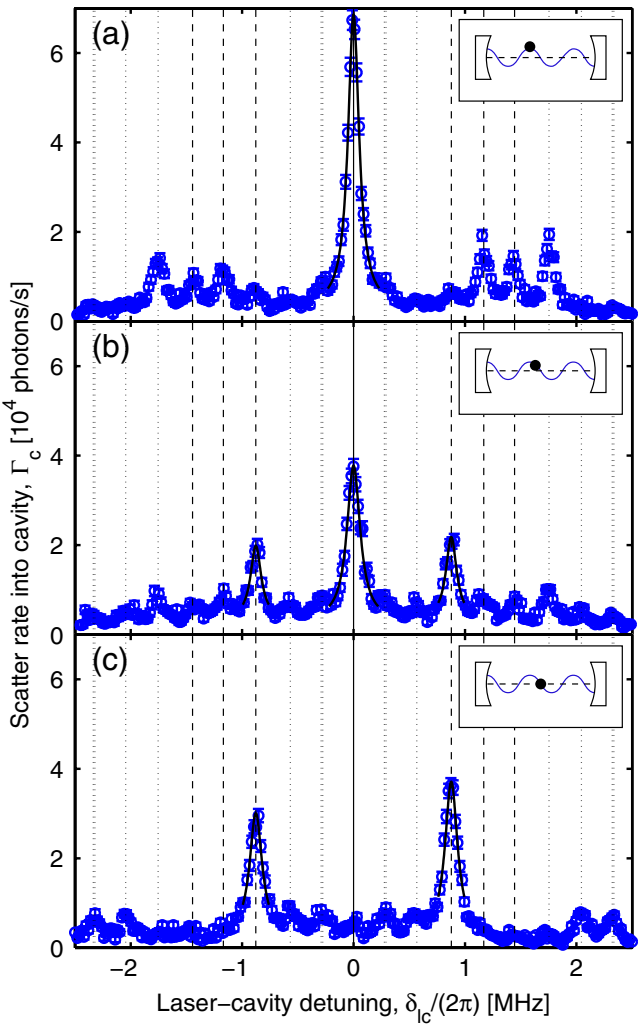


FIG. 3 (color online). Photon scattering rate into the cavity as a function of laser-cavity detuning δ_{lc} with the ion located at a cavity standing-wave antinode (a), halfway between a node and an antinode (b), and at a node (c). Each data point is measured by preparing the ion at fixed temperature by Doppler cooling for 200 μ s, then measuring the rate of scattering photons from the cavity cooling beam into the cavity for 50 μ s with $\delta_{ci}/(2\pi) = -60$ MHz and $\Gamma_{sc} = 1.2 \times 10^7$ photons/s. The solid, dashed, and dotted vertical lines are at the carrier, first-order motional sideband, and second-order motional sideband transition frequencies, respectively. The curves are Lorentzian fits with linewidths consistent with the combined linewidth of the cavity and laser.

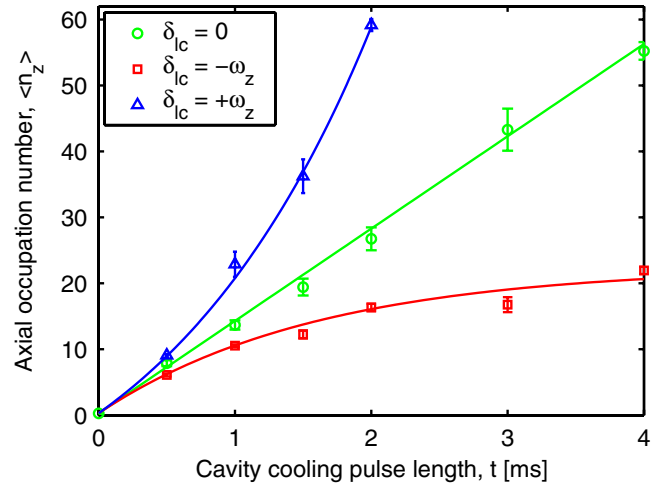


FIG. 4 (color online). Cavity cooling dynamics. The ion is sideband cooled to the three-dimensional motional ground state; a cavity cooling pulse with detuning $\delta_{lc} = 0$ (carrier), $\delta_{lc} = -\omega_z$ (red axial sideband), or $\delta_{lc} = +\omega_z$ (blue axial sideband) is applied; and the mean number of motional quanta in the z mode is measured. The three lines are a simultaneous fit to the model described in the supplementary information [23] with fit parameters $n_0 = 0.30(6)$, $\Gamma_{sc} = 2.87(2) \times 10^6$ photons/s, and $\eta = 0.0148(2)$. The reduced χ^2 of the fit is 1.7.

the temperature after pumping on the cavity red sideband is smaller than the temperature after pumping on the cavity carrier, which is smaller than the temperature after pumping on the cavity blue sideband. Cavity cooling ($\delta_{lc} = -\omega_z$) counteracts recoil heating by free-space scattering, and results in a finite steady-state vibrational quantum number $n_\infty \approx 20$.

We fit the cavity cooling dynamics to a rate equation model parameterized by the initial mean occupation number n_0 , the free-space scattering rate Γ_{sc} , and the effective cooperativity η [9] (see the supplementary information for details [23]). The data in Fig. 4 fits the model with fit parameters $n_0 = 0.30(6)$, $\Gamma_{sc} = 2.87(2) \times 10^6 \text{ s}^{-1}$, and $\eta = 0.0148(2)$ with a reduced χ^2 of 1.7. These values of the fit parameters are equally consistent with those derived from independent direct measurements (the reduced χ^2 between the data and the model using the independently measured values of the parameters is 2.0), so that the rate equation model describes our data without any free parameters. The steady-state mean occupation number due to cavity cooling is limited by the relatively small cooperativity of the cavity to $n_\infty = 22.5(3)$.

In conclusion, we have demonstrated one-dimensional cavity cooling of a single $^{88}\text{Sr}^+$ ion in the resolved-sideband regime. While our small effective cooperativity prevents us from cooling to the motional ground state, we have observed clearly resolved motional sidebands in the cavity emission spectrum, and we have measured the cavity cooling and heating rates. Our results validate the rate equation model proposed by Vuletić *et al.* [8,9], which predicts that it is possible to cavity cool atoms or ions to the motional ground state without decohering the internal state. This would require a large detuning of the laser compared to the atomic fine structure, a criterion which is easier to meet with light ions such as Be^+ [12].

Resolved-sideband cavity cooling might also be used to cool large molecular ions to the motional ground state [24,25]. While some species of molecular ions have been previously cooled using sympathetic cooling [26–28], large mass ratios between the atomic cooling ions and the molecular ions prevent efficient sympathetic cooling of the molecular ions at temperatures near the motional ground state. Resolved-sideband cavity cooling could enable exciting new studies of large molecular ions in the quantized motional regime.

We thank S. Urabe for providing the linear RF Paul trap used in this work and J. Simon, M. Cetina, and A. Grier for advice. This work is supported in part by the Japan Science and Technology Agency, the NSF, and the NSF Center for Ultracold Atoms.

*dleibran@mit.edu

[1] F. Diedrich, J.C. Bergquist, W.M. Itano, and D.J. Wineland, Phys. Rev. Lett. **62**, 403 (1989).

- [2] S. E. Hamann, D. L. Haycock, G. Klose, P. H. Pax, I. H. Deutsch, and P. S. Jessen, Phys. Rev. Lett. **80**, 4149 (1998).
- [3] C. F. Roos, D. Leibfried, A. Mundt, F. Schmidt-Kaler, J. Eschner, and R. Blatt, Phys. Rev. Lett. **85**, 5547 (2000).
- [4] A. Schliesser, R. Rivière, G. Anetsberger, O. Arcizet, and T. J. Kippenberg, Nature Phys. **4**, 415 (2008).
- [5] D. J. Wineland, C. Monroe, W. M. Itano, D. Leibfried, B. E. King, and D. M. Meekhof, J. Res. Natl. Inst. Stand. Technol. **103**, 259 (1998).
- [6] J. P. Home, M. J. McDonnell, D. J. Szwer, B. C. Keitch, D. M. Lucas, D. N. Stacey, and A. M. Steane, arXiv:0810.1036.
- [7] P. Horak, G. Hechenblaikner, K. M. Gheri, H. Stecher, and H. Ritsch, Phys. Rev. Lett. **79**, 4974 (1997).
- [8] V. Vuletić and S. Chu, Phys. Rev. Lett. **84**, 3787 (2000).
- [9] V. Vuletić, H. W. Chan, and A. T. Black, Phys. Rev. A **64**, 033405 (2001).
- [10] T. Hänsch and A. L. Schawlow, Opt. Commun. **13**, 68 (1975).
- [11] R. A. Cline, J. D. Miller, M. R. Matthews, and D. J. Heinzen, Opt. Lett. **19**, 207 (1994).
- [12] R. Ozeri *et al.*, Phys. Rev. Lett. **95**, 030403 (2005).
- [13] P. Maunz, T. Puppe, I. Schuster, N. Syassen, P. W. H. Pinkse, and G. Rempe, Nature (London) **428**, 50 (2004).
- [14] S. Nußmann, K. Murr, M. Hijkema, B. Weber, A. Kuhn, and G. Rempe, Nature Phys. **1**, 122 (2005).
- [15] K. M. Fortier, S. Y. Kim, M. J. Gibbons, P. Ahmadi, and M. S. Chapman, Phys. Rev. Lett. **98**, 233601 (2007).
- [16] H. W. Chan, A. T. Black, and V. Vuletic, Phys. Rev. Lett. **90**, 063003 (2003).
- [17] A. T. Black, H. W. Chan, and V. Vuletic, Phys. Rev. Lett. **91**, 203001 (2003).
- [18] G. R. Guthöhrlein, M. Keller, K. Hayasaka, W. Lange, and H. Walther, Nature (London) **414**, 49 (2001).
- [19] A. B. Mundt, A. Kreuter, C. Becher, D. Leibfried, J. Eschner, F. Schmidt-Kaler, and R. Blatt, Phys. Rev. Lett. **89**, 103001 (2002).
- [20] C. Russo *et al.*, Appl. Phys. B **95**, 205 (2009).
- [21] P. F. Herskind, A. Dantan, J. P. Marler, M. Albert, and M. Drewsen, Nature Phys. **5**, 494 (2009).
- [22] J. I. Cirac, R. Blatt, P. Zoller, and W. D. Phillips, Phys. Rev. A **46**, 2668 (1992).
- [23] See EPAPS Document No. E-PRLTAO-103-072935 for a description of the rate equation model of cavity sideband cooling. For more information on EPAPS, see <http://www.aip.org/pubservs/epaps.html>.
- [24] B. L. Lev, A. Vukics, E. R. Hudson, B. C. Sawyer, P. Domokos, H. Ritsch, and J. Ye, Phys. Rev. A **77**, 023402 (2008).
- [25] G. Morigi, P. W. H. Pinkse, M. Kowalewski, and R. de Vivie-Riedle, Phys. Rev. Lett. **99**, 073001 (2007).
- [26] K. Mølhave and M. Drewsen, Phys. Rev. A **62**, 011401(R) (2000).
- [27] V. L. Ryjkov, X. Z. Zhao, and H. A. Schuessler, Phys. Rev. A **74**, 023401 (2006).
- [28] A. Ostendorf, C. B. Zhang, M. A. Wilson, D. Offenberg, B. Roth, and S. Schiller, Phys. Rev. Lett. **97**, 243005 (2006).